applied sciences

MDPI

Article

The Effect of Dynamic Injurious Axial Impact on Human Cervical Intervertebral Disc Pressure Response: Methodology & Initial Results

Sara Sochor [1,*], Mark R. Sochor [2], Juan M. Asensio-Gil [1], Carlos Rodríguez-Morcillo García [1] and Francisco J. Lopez-Valdes [1]

[1] MOBIOS Lab, Institute for Research in Technology, Comillas Pontifical University, C. Alberto Aguilera 23, 28015 Madrid, Spain; jasensio@comillas.edu (J.M.A.-G.); carlosrg@comillas.edu (C.R.-M.G.); fjlvaldes@comillas.edu (F.J.L.-V.)

[2] Center for Applied Biomechanics, Department of Mechanical and Aerospace Engineering, University of Virginia, 4040 Lewis and Clark Dr., Charlottesville, VA 22911, USA; ms7ha@uvahealth.org

* Correspondence: sara.sochor@alu.comillas.edu

Featured Application

This study presents a methodology-focused biomechanical investigation into human cervical intervertebral disc (CIVD) pressure responses during dynamic injurious axial head–neck impacts using post-mortem human subjects (PMHS, i.e., cadavers). Results provide confidence in the linkage between observed changes in CIVD pressure and cervical spine failure under these loading conditions.

Abstract

Cervical spine (c-spine) injuries are a prominent concern in sporting activities, and dynamic axial (i.e., head-first) impacts are associated with a high risk of c-spine trauma. This methodology study implanted pressure sensors in post-mortem human subject (PMHS) cervical intervertebral discs (CIVDs) to assess biomechanical response and disc pressure changes during dynamic injurious axial impacts. Two fresh frozen male head–neck PMHS (cephalus with complete c-spine) were instrumented with miniature pressure sensors (Model 060S, Precision Measurement Company, Ann Arbor, MI, USA) at three CIVD levels (upper, middle, and lower c-spine). Experiments replicated the Nightingale et al. studies, simulating a rigid unconstrained head vertex (0°) axial impact. PMHS were raised to a drop height of 0.53 m to reach the desired impact velocity of ~3.2 m/s and were allowed to drop vertically. Results showed characteristic c-spine deformations/buckling motion patterns and marked CIVD pressure differences between CIVD levels. The more cranial (C2–C4) and caudal (C6–T1) CIVD exhibited greater and more comparable pressure values than those of the mid-spine (C4–C6), and the pressure in upper/lower levels was at least ~four to six times higher than that of the middle. This study establishes the feasibility and assesses the potential of CIVD pressure as a biomechanical metric for assessing injurious axial loading and contributes a novel experimental framework for future injury tolerance research and model validation.

Keywords: biomechanics; cervical spine; neck; intervertebral disc; axial impact; cadaver; PMHS; pressure; dynamic; injury prevention

Academic Editor: Jorge Sánchez-Infante

Received: 5 December 2025
Revised: 5 January 2026
Accepted: 7 January 2026
Published: 14 January 2026

1. Introduction

Cervical spine (c-spine) injuries are a prominent concern in the fields of biomechanics and sports injury prevention. Sports participation is the fourth most common cause of neck trauma (following motor vehicle-related incidents, violence, and falls [1]), and the third most common cause of spinal cord injury (SCI) (following motor vehicle incidents and violence) [2]. The National Spinal Cord Injury Statistical Center reports an incidence of approximately 18,000 new traumatic cervical SCI patients per year [3], with ~82% of all sports-related SCI resulting in tetraplegia. Sporting event related incidence rates vary considerably between global regions and with degree of participation/contact due to the wide variability in popularity and type of sport played around the world [4]. While the percentages greatly vary depending on factors such as the severity of the insult, the demographics of the injured individuals, and injury severity, American football, hockey, rugby, gymnastics, skiing and swimming/diving are prominent sources of c-spine trauma and cervical SCI in athletes globally [2,4–8].

More severe/destructive c-spine injuries (e.g., vertebral fractures/dislocations, disc injuries, and/or spinal cord injuries resulting in catastrophic neurological deficits) are most common among collision sports and typically occur as a result of head-contact/impacts in which the head motion is arrested and the neck is forced to stop the mass of the moving torso [9,10]. In this configuration, head impact velocities as low as 3.1 m/s (equivalent to falling from a height of 0.5 m) have been reported as adequate to produce c-spine injury, with injury risk increasing with increased head motion constraint [6,11,12]. These axial (i.e., head-first) impacts constitute a relatively infrequent occurrence in athletes, but are serious/severe (Abbreviated Injury Scale [13], AIS 3+) c-spine trauma and are a leading cause of serious neck injury with devastating neurological consequences [4–6,14–18]. Understanding the frequency of c-spine injury is confounded by the difficulty in diagnosing these injuries, particularly in the upper c-spine (e.g., the craniocervical junction) [4,19], and these numbers may be subject to underestimation due to high pre-admission mortality rates related to this type of injury [20,21].

While the incidence of catastrophic sports-related c-spine trauma has been significantly reduced over the past ~50 years, the injury warrants continued attention due to the quality of life alterations that often result from such traumatic insults [16,17]. Ongoing advancements in sports safety technology and injury prediction and prevention tools continue to play a crucial role in evaluating traumatic insults to the c-spine. Many research initiatives have made positive efforts to evaluate c-spine kinematics, forces/loads, and resultant tolerance limits/injury mechanisms [1,11,12,22–32]; yet it is still abundantly clear that experimental instrumentation of the c-spine for data capture is an anatomical challenge. As a result of these data capture limitations, current neck injury corridors are primarily derived from live human volunteer data and are almost purely established from head motion characterizations [33,34] (despite head motions have been shown to *not* be predictive of local c-spine injury mechanism [11]), as opposed to true biomechanical tissue responses of the c-spine itself. In previous studies, instrumentation for c-spine data capture is limited to the two farthest anatomical neck boundaries, the head and the torso, consequently forcing oversimplification in the design and resultant biofidelity of current human surrogates for injury biomechanics testing. The c-spine of current anthropometric test devices (i.e., ATDs, i.e., "crash test dummies") exhibit an utter lack of true spinal segments/curvature, and load cells situated within the head/upper torso of record forces and moments at *only* the upper neck (i.e., C1/skull occiput) and lower neck (i.e., first thoracic vertebrae).

There has not yet been a robust attempt to characterize the biomechanical response of the individual c-spine levels *between* the two anatomical neck boundaries (i.e., the upper neck and lower neck in a dynamic axial loading mode. Intervertebral disc (IVD)

pressure measurements are the most direct method of estimating spinal loads and have been utilized in spine biomechanics work for 50+ years (albeit, predominantly in the lumbar spine region [35–39]). IVD pressure sensors are capable of recording pressure that can be correlated to load, especially under compressive loading conditions [39–41]. While the most direct method of quantifying loads transmitted through the anterior c-spine is to measure the pressure in the cervical disc center (i.e., the nucleus pulposus), there has not yet been a robust attempt to characterize the biomechanical response of *cervical* intervertebral discs (CIVDs) within the complete head–neck complex PMHS.

Biomechanical studies establishing a relationship between CIVD tissue response (i.e., changes in pressure) and c-spine motion/loading are not well represented in the current literature (Appendix A). Only two fundamental in vivo studies (i.e., research performed on a living human) have been identified, together providing the first in vivo head/neck motion related CIVD pressure values in normal/abnormal discs [42,43]). In vitro (i.e., laboratory-based research) studies largely report data from testing with small component PMHS specimens (e.g., independent c-spines, c-spine functional spinal units (FSUs)). Two predominant in vitro studies form the basis for many subsequent in vitro/PMHS-based CIVD biomechanics studies. Pospiech et al. [44] was the first to measure IVD pressure in the c-spine in an in vitro/experimental setting and sought to establish normal values for CIVD pressures under "physiological conditions" with and without simulated muscle forces. Cripton et al. [41] developed a minimally invasive technique for measuring CIVD pressure in vitro utilizing miniature pressure transducers (Model 060 S, Precision Measurement Co., Ann Arbor, MI, USA) and established that there exists a linear relationship between CIVD pressure and (purely) compressive force. In all aforementioned studies, CIVD pressure responses were evaluated under quasistatic conditions, and in vivo experimentation was based on smaller PMHS components (e.g., FSUs [41]), and/or in a purely clinical/surgical setting [45–55]. Existing dynamic head–neck injury research is well established [56], albeit sans CIVD pressure measurements. Thus, the exact relationship of CIVD pressures to dynamic head/neck loading remains uncertain.

The primary goal of this methodology study was to replicate the hallmark human c-spine injury biomechanics experimentation conducted by Nightingale et al. [11,12] with the addition of CIVD pressure sensor instrumentation to establish a novel methodology for assessing the ability of miniature pressure sensors to detect changes in CIVD pressure during dynamic injurious axial impacts in PMHS head/neck specimens. To our knowledge, implanting pressure sensors into the CIVDs of complete c-spine PMHS (i.e., cephalus with complete c-spine) for *dynamic* injurious impact testing and c-spine injury tolerance has not been previously reported in the biomechanics literature. Based on the results from previous feasibility work [57], we hypothesize that CIVD pressure sensors can both detect and define the transmission/propagation of *injurious* load/forces along the *entire* c-spine (versus data capture at only at the anatomical limits). This successive methodology study investigates the potential applicability of CIVD pressures to c-*spine injury tolerance* in *dynamic* test environments, to contribute a novel experimental framework for future injury tolerance research and model validation.

2. Materials and Methods

2.1. Experimental System

To investigate the potential applicability of CIVD pressures as a biomechanical metric for assessing injurious axial loading, we replicated the dynamic axial human c-spine injury biomechanics experimentation conducted by Nightingale et al. [11,12] with the addition of CIVD pressure sensor instrumentation. As in the Nightingale studies [11,12], a vertical drop test system was constructed to simulate an axial head impact with a following torso

load, while controlling for initial PMHS positioning, drop height, and impact surface orientation (Figure 1).

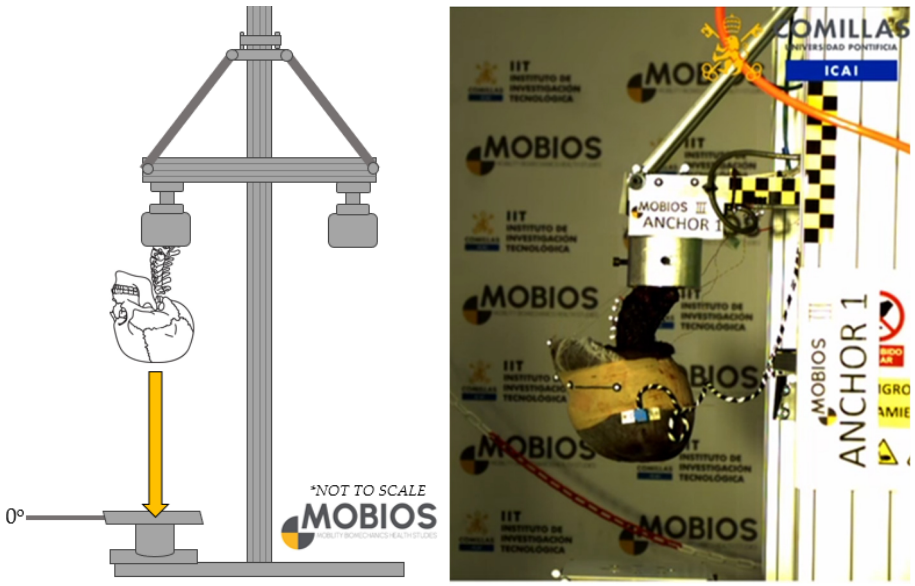

(a) (b)

Figure 1. (**a**) MOBIOS vertical drop test system designed to replicate c-spine experimentation conducted by Nightingale et al. [11,12] (**b**) MOBIOS pilot experimental system designed to investigate CIVD pressure responses during injurious dynamic axial impacts in component head–neck PMHS.

A self-designed vertical drop tower test fixture was comprised of two linear rails with bushing sliders and a total carriage and counterweight aimed to approximate the weight of a fiftieth percentile male effective upper torso mass (~16 kg) [11,12]. The impact surface consisted of a Teflon covered steel plate positioned under the PMHS skull apex to simulate a rigid unconstrained vertex (0°) head impact. A six-axis load cell was installed at each end of the test apparatus to measure forces/moments at both the neck and head (MC3A-1000 and MC5-10000 respectively; AMTI, Watertown, MA, USA). A digital data acquisition system (DTS Slice Micro with DataPRO software (Version: 4.0.752; DTS, Seal Beach, CA, USA) recorded data from accelerometers, load cells, and pressure sensors at 20,000 Hz. A three-dimensional (3D) motion capture system (Vicon Motion System, Kidlington, UK) recorded specimen kinematics at 1000 Hz. Experiments were imaged at 2000 frames per second (FASTCAM SA3; Photron, Bucks, UK). Data analysis was performed in META post-processor software (Version: 24.0.1; BETA CAE Systems, Davos-Platz, CH).

2.2. Specimen Preparation

Four fresh frozen mid-size (~fiftieth percentile) male component head–neck PMHS (i.e., cephalus with complete c-spine/through the fourth thoracic vertebrae (T4)) (Figure 2) were procured according to the procedures established at MOBIOS Lab and received approval from the Universidad Pontificia Comillas Ethics Committee (Dictamen 006/25-26). All experimental procedures were performed according to the principles outlined in the Declaration of Helsinki (1975, revised in 2013), national regulations in Spain, international best ethical practices [58], and in accordance with the guidelines established by the Human Usage Review Panel of the US National Highway Traffic Safety Administration (NHTSA). PMHS were pre-screened for bloodborne pathogens and handled using universal precautions per laboratory safety guidelines. Demographic and anthropometric information (i.e., sex, age, height, weight, and cause of death) was collected for each PMHS (Table 1), and medical histories/initial computed tomography (CT) images were reviewed to rule out

anatomical anomalies, prior surgical intervention/hardware, and/or evidence of spine disease/pathology. One specimen (PMHS 1, 0047M) exhibited tissue degradation and cervical lordosis rectification (i.e., straightening) related to antemortem illness and clinical treatment, and another (PMHS 2, 0042M) had previously been utilized for biomechanical testing with consequent post-test injuries, rendering the specimen a non-viable candidate for this series; thus, PMHS 1 and 2 acted as experimental pilots for purely methodology and test fixture/instrumentation modulation only. Two of the four subjects (PMHS 3, 0038M; PMHS 4, 0037M) were deemed to have acceptable cervical vertebrae and IVDs with limited (age appropriate) degeneration (Figure 2).

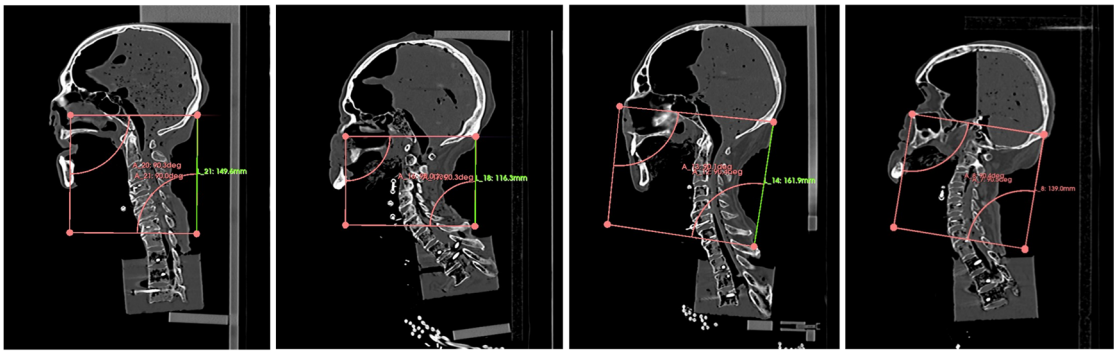

PMHS 1 0047M | **PMHS 2** 0042M | **PMHS 3** 0038M | **PMHS 4** 0037M

Figure 2. Four fresh frozen mid-size male component head–neck (i.e., cephalus with complete c-spine/through the fourth thoracic vertebrae (T4)) PMHS.

Table 1. PMHS demographic and anthropometric information.

PMHS #	MOBIOS Donor ID	Sex	Age [Years]	Cause of Death
1	0047M	Male	63	Supraglottic cancer
2	0042M	Male	63	Global respiratory failure
3	0038M	Male	71	Cardiorespiratory failure
4	0037M	Male	68	Respiratory failure

Head/Neck Anthropometry [cm]	PMHS 1	PMHS 2	PMHS 3	PMHS 4
Head circumference	52.0	55.5	55.8	53.3
Head length	18.5	20.0	20.0	19.0
Head breadth	13.8	14.5	14.8	14.5
Head height	23.0	24.5	22.0	20.9
Neck circumference	39.0	N/A [1]	43.5	40.0
Total specimen length [2]	12.0	15.5	15.0	16.5
Total specimen height [3]	36.0	38.5	35.5	37.0

[1] Exact measurement not available due to previous soft tissue dissection/removal. [2] Occiput to T1 spinous process. [3] Top of head to bottom of pot.

PMHS were preserved frozen at ~−20 °C until needed and thawed for ~24 h at room temperature prior to instrumentation and subsequent experimentation. Limited soft tissue was removed from the PMHS to maintain natural anatomical influence of surrounding structures; in contrast to previous studies in which the PMHS was dissected down to an osteoligamentous structure [11,12], posterior neck musculature was left intact while only anterior soft tissue throat structures (i.e., pharynx, larynx, trachea, and esophagus) were removed (with minimal disruption of anterior deep neck musculature) to increase anterior c-spine visibility. The three caudal-most thoracic vertebrae (T2–T4) were denuded and potted in an aluminum cup with ultra-low viscosity casting resin, taking care to maintain

the neutral first thoracic vertebrae (T1) angle (25°) [59] and to ensure the C7–T1 motion segment was not hindered by the potting material. The potting cup was cooled in a water bath during the exothermic resin curing reaction to mitigate specimen degradation.

Instrumentation for data capture in the c-spine requires specialized surgical techniques and miniature-scale data acquisition tools to provide practical data due to dynamic anatomical space limitations. As in preceding pilot experimentation, miniature pressure sensors (Model 060S, range 0–3450 kPa, Precision Measurement Company) were chosen for the proposed experimentation for their small size (3.0 mm length × 1.5 mm width × 0.3 mm thickness) and ability to withstand the post-mortem soft tissue environment [57]. This pressure transducer was previously used to record CIVD pressures in PMHS FSUs by Cripton et al. [41] and others in a more clinical/surgical setting [45–55]. Prior to sensor use, a plausibility check was conducted to confirm pressure sensor calibration linearity. An initial CT scan was used to determine specimen-specific anatomy to plan for pressure sensor insertion point/depth to maximize sensor placement at the disc center, i.e., nucleus pulposus [39]. Each PMHS was instrumented with three miniature pressure sensors using a specialized and minimally invasive surgical technique [57], with one sensor implanted at a location within each of three designated CIVD levels (i.e., upper/C2–C4, middle/C4–C6, and lower/C6–T1 c-spine level) (Figure 3).

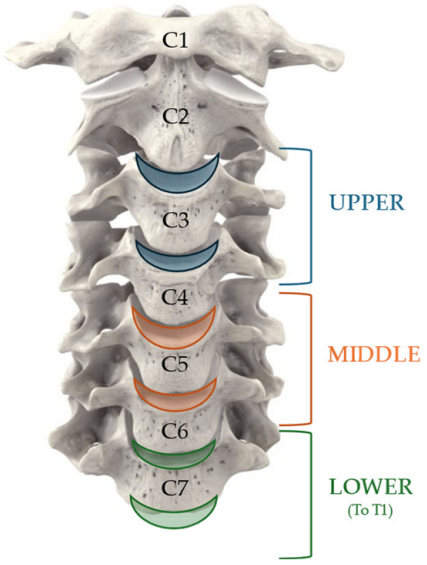

Figure 3. Each PMHS was instrumented with three miniature pressure sensors, with one sensor implanted in the CIVD at each of three designated CIVD levels (i.e., upper/C2–C4 (blue), middle/C4–C6 (orange), and lower/C6–T1 (green) c-spine level). Image adapted from Anatomy Standard, 2021–2025.

3D motion tracking arrays with reflective spherical markers were installed anteriorly at multiple cervical vertebral levels and additional surface markers provided supplemental anatomical landmarks for 3D tracking analysis. A six degree-of-freedom sensor package (6DX PRO-A 500G; DTS, Seal Beach, CA, USA), was installed on the lateral skull (parallel to the Frankfurt plane) to measure head–neck angular displacement. PMHS underwent post-instrumentation CT (0.65 mm slice thickness × 0.65 mm slice interval) to confirm both instrumentation placement and the neutral T1 potted angle of ~25°, and then again post-test to radiographically identify injury.

2.3. Test Protocol

Specimen positioning was performed to replicate and facilitate comparison with previous Nightingale et al. tests [11,12]. Potted PMHS were preconditioning via multiple cycles of manual head/neck exercise and then placed in an inverted neutral head/neck posture (i.e., Frankfurt horizontal plane parallel to the ground and neutral T1 angle of ~25° sagittal to the ground), thus preserving resting cervical lordosis. A single break-away suture (passed around the mandible and attached to the mobile portion of the test fixture) was implemented to maintain the neutral orientation of the specimen prior to drop. Specimens were raised to the drop height of 0.53 m in order to reach the desired impact velocity of ~3.2 m/s (chosen to produce c-spine injury sans skull fracture [6,11]). Specimen-specific axial deflection limits (i.e., stroke) were applied, as in a previous Nightingale study [60], with the magnitude of applied displacement scaled based on a specimen length ratio. The PMHS were released and allowed to drop vertically, sustaining head vertex (0°) impact with the load plate below. Each PMHS was subjected to a single experimental drop; repeat drops per specimen were considered but intentionally avoided to prevent cumulative damage and/or microinjury. Post-test CT imaging and subsequent dissection determined the extent/type of injury sustained.

3. Results

Due to the limitations and subsequent experimental exclusion of specimens PMHS 1 and PMHS 2 (as described in the methods), numerical results from PMHS 3 and PMHS 4 are reported here. Both PMHS (PMHS 3 and PMHS 4) generated viable test data, in which cervical kinematics and CIVD pressure readings were successfully obtained for all instrumented c-spine levels. Characteristic c-spine deformations/buckling motion patterns related to dynamic axial loading were observed upon head impact (Figure 4). The PMHS exhibited similarly shaped head and neck force peaks, as well as similarly shaped CIVD pressure peaks (magnitude and time) despite slightly different CIVD instrumentation levels. The more cranial (C2–C4) and caudal (C6–T1) CIVD levels exhibited greater and more comparable pressure values than those of the mid-spine disc level (C4–C6), and the pressure in upper/lower levels was ~four to six times higher than that of the middle (Table 2). Unfortunately, this increase resulted in pressure sensor saturation for upper and lower CIVD levels in both PMHS; therefore, the pressure values at the time of saturation (i.e., maximum pressure recorded) are reported here.

Table 2. Summary of peak axial head/neck forces and peak * CIVD pressure values for PMHS 3 (0038M) and PMHS 4 (0037M). * Pressure sensor saturation occurred in upper and lower CIVD levels in both PMHS; therefore, the maximum pressure value at the time of saturation is reported here.

PMHS 3 (0038M)		PMHS 4 (0037M)	
	Force (N)		***Force (N)***
Head Z	3812.7	**Head Z**	5648.2
Neck Z	1750.5	**Neck Z**	1145.4
	Pressure (kPa)		***Pressure (kPa)***
Upper (C3C4)	1871.6 *	**Upper (C2C3)**	3093.8 *
Middle (C4C5)	1108.1	**Middle (C4C5)**	184.5
Lower (C7T1)	5217.6 *	**Lower (C6C7)**	2566.9 *

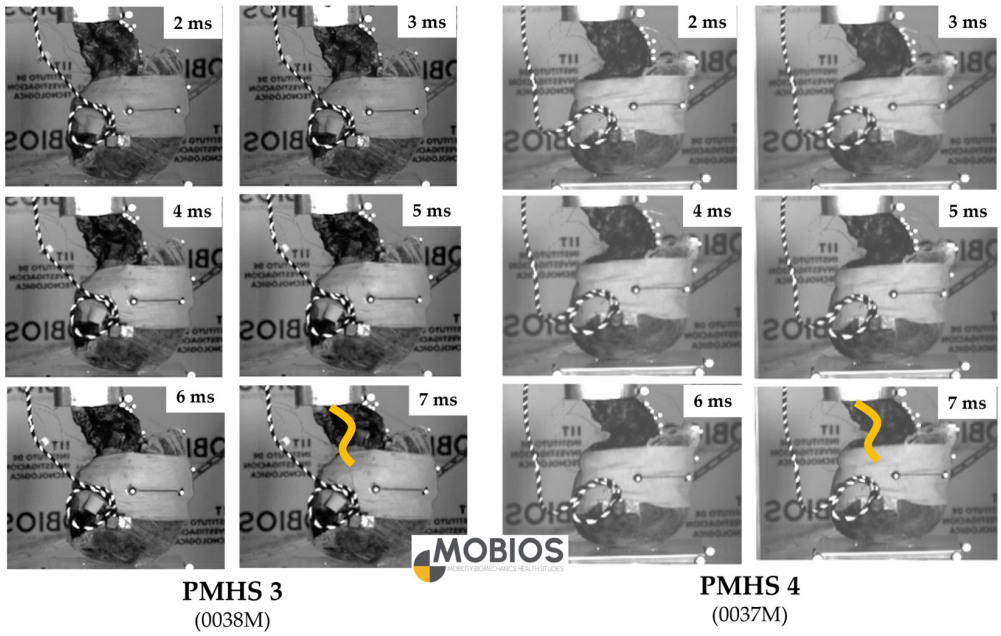

Figure 4. Highspeed video frames for PMHS 3 (0038M, **left**) and PMHS 4 (0037M, **right**) revealed the characteristic c-spine axial deformation [11] with initial serpentine deformation (~three ms) followed by a rapid shift into "buckling" (yellow line) comprising extension in the upper (~third through fifth) cervical motion segments and flexion of the lower (~sixth through seventh cervical/first thoracic) vertebral motion segments (~7 ms).

For both PMHS, force and pressure progression occurred in a way that is consistent with the experimental condition of dynamic axial loading. Upon head contact with the impact surface, specimen head Z forces peaked first, followed by upper then lower CIVD pressures. After a short lag, the middle CIVD pressure increased slightly before/concomitant with the neck Z force (Figure 5). As is the "standard" in biomechanics experimentation, a decrease in axial load with continued axial compression/c-spine deformation (the "traditional definition of failure") was used to define c-spine failure/injury [11]. CIVD pressure increases occurred prior to the sudden drop in axial neck load (i.e., the moment of c-spine failure; Figure 6, yellow star), but the exact pressure sensor trends occurring at c-spine failure were unobtainable due to upper and lower CIVD pressure sensor saturations. Overall data trends and peak axial neck force were comparable to previous Nightingale studies [11,12] as were the resultant c-spine injuries (Appendix B). In tandem with the sudden decrease in axial neck load, radiographic post-test imaging identified positive c-spine injury associated with an axial load to the head/neck. One PMHS (PMHS 4, 0037M) sustained a type III Jefferson (C1) fracture and a C3 vertebral body fracture (Figure 7), while the other PMHS (PMHS 3, 0038M) displayed a type II dens (C2) fracture, all correlate with preceding increases in CIVD pressure.

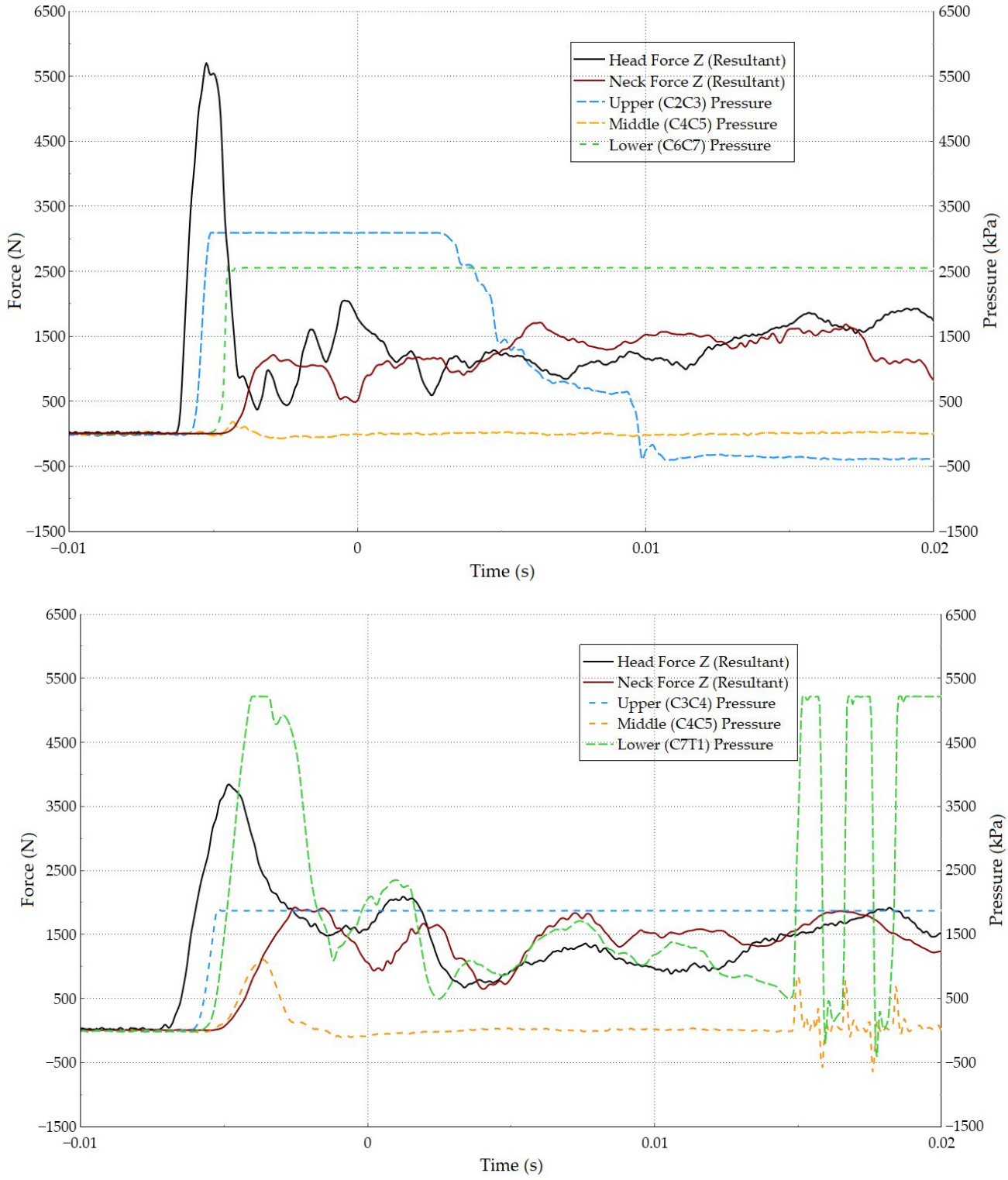

Figure 5. Results for PMHS 4 (0037M, **top**) and PMHS 3 (0038M, **bottom**) show comparable data trends for both head/neck force and CIVD pressure response. Individual data traces are included in Appendix C.

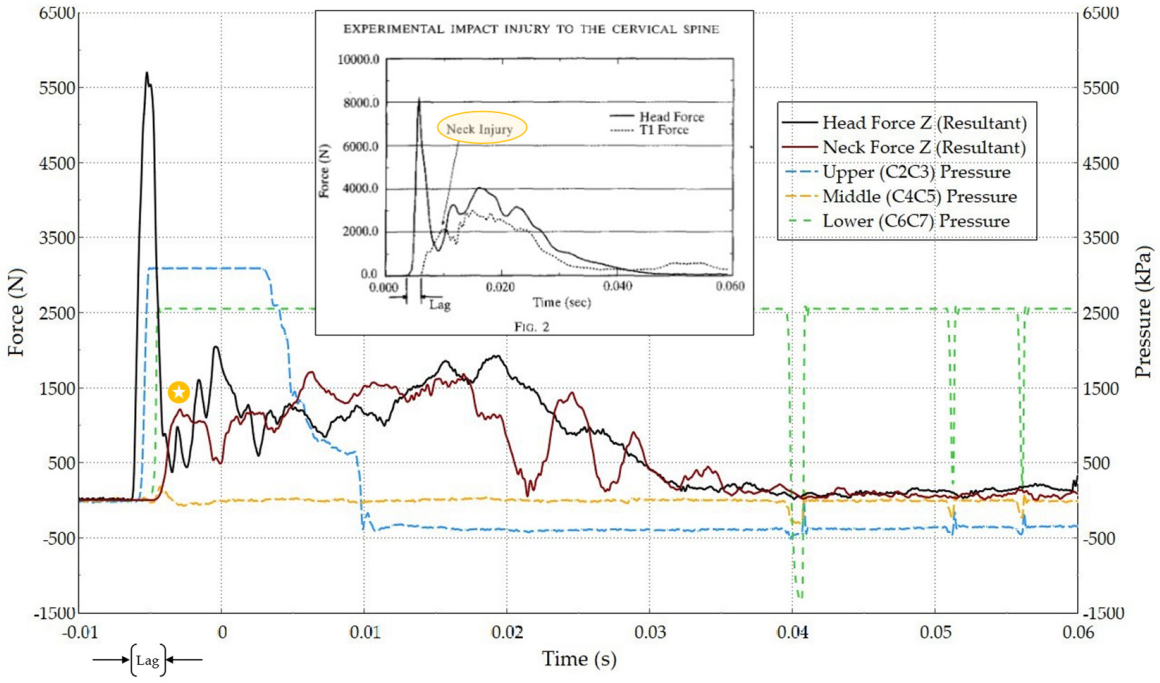

Figure 6. Results for PMHS 4 (0037M) show comparable data trends between MOBIOS experimentation and Nightingale testing (inset, results from Nightingale et al. [12]). Yellow star indicates a sudden decrease in neck load, assumed to identify occurrence of c-spine failure/injury (yellow circle in inset).

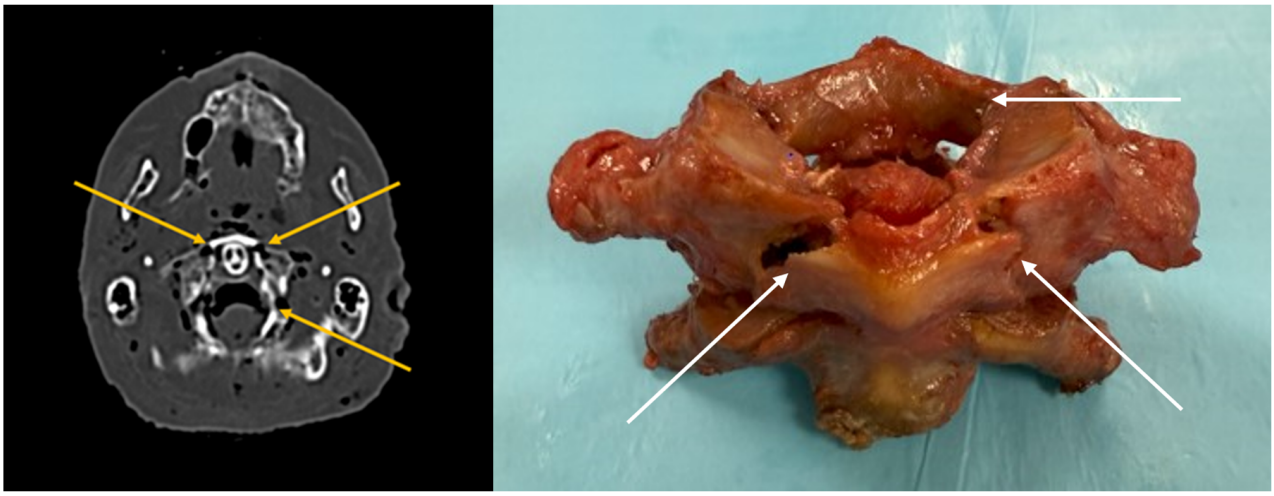

(**a**) (**b**)

Figure 7. Post-test injury identification for PMHS 4 (0037M) revealed a type III Jefferson injury (C1, fractures denoted by arrows) on both post-test CT (**a**) and post-test dissection (**b**).

4. Discussion

The primary goal of this study was to replicate the hallmark c-spine injury biomechanics experimentation conducted by Nightingale et al. [11,12] while establishing a methodology for assessing the ability of miniature pressure sensors to detect changes in CIVD pressure during dynamic axial impacts to the head/neck complex. We successfully built upon the Nightingale et al. studies [11,12] with the addition of CIVD pressure sensor instrumentation, which could be an initial step in assessing CIVD pressure as a novel biomechanical metric for assessing injurious axial loading. To our knowledge, this is the first study to implement the use of miniature pressure sensors in component PMHS

cephalus with complete c-spine CIVDs to assess pressure changes during *dynamic* injurious axial impact c-spine testing for biomechanical response. This pilot experimentation showed promising results lending credence to our hypothesis that CIVD pressure sensors can both detect and begin to define *injurious* dynamic axial load on PMHS head-c-spine specimens, providing confidence in the linkage between observed changes in CIVD pressure and failure in axial loading. A total of four specimens (experimental specimens PMHS 3 and 4, as well as PMHS 1 and PMHS 2 used purely for test fixture/instrumentation modulation) were sufficient for methodological validation; however, all findings are considered preliminary and no statistical inference is intended, only feasibility and trend identification.

Our secondary goal was to evaluate if our methodology and instrumentation (which built upon and/or differed substantially from many of the previous studies) proffered viable pressure trends. Cripton et al. [41] showed that CIVD pressure varied linearly with applied axial compression and provided a gross "rule of thumb" for CIVD pressure estimation in which ~3750 kPa of pressure is induced per 1000 N of compression; however, it is important to note the critical differences between this testing and the current study. Cripton et al. [41] provided the abovementioned pressure guidelines based on data extrapolation from testing in which simple PMHS FSUs (i.e., two human cervical vertebrae and the single CIVD between) were subjected to pure axial compression forces at a rate of 10 N/s under force control, up to 800 N. Conversely, the current study utilized large component head/entire c-spine component PMHS in which there were multiple motion segments giving rise to complex deformations (i.e., independent motion/variability between the individual intervertebral levels due to the segmented nature of the spine) along the entire c-spine during the dynamic (~3.2 m/s) application of much higher forces (3000+ N). Employing the use of CIVD pressure sensors in a larger component PMHS provided a more realistic head/neck complex response and acts as a firm experimental base for our feasibility study. Additionally, the Cripton study was quasistatic (10 N/s, up to 800 N) and these experiments were dynamic. Thus, in this dynamic experimental environment, the purely linear CIVD pressure response for all tested c-spine levels as described by Cripton et al. [41] was not directly observed.

Results from the current study did seem to align with the pressure values expressed by Cripton et al. for the upper c-spine levels (i.e., C2–C4); however, the mid-spine disc level (i.e., C4–C6) did not exhibit the same properties and demonstrated much lower pressure values. Also, the current experimental protocol resulted in a state of combined loading in which axial compression resulted in bimodal bending with concomitant extension (in the upper) and flexion (in the lower) c-spine, consistent with the characteristic c-spine deformations/buckling motion patterns observed during axial impacts [11]. Previous studies have shown the miniature pressure sensors utilized in this study are indeed able to detect changes in combined spinal loading states (e.g., combined compression and flexion [39]), such as those observed during the current study. Differentiating the exact effects of each component in this combined loading condition on CIVD pressure response remains the focus of future work.

In patients surviving traumatic insults to the c-spine, injury is most common in the mid-c-spine, typically between the C4 and C6 vertebrae [4]. Data from the preceding quasistatic CIVD pressure response pilot study [57] and previous literature examining the pressure response for other neck tissues/areas (i.e., intrathecal cerebrospinal fluid [61]) show greater peak pressure and pressure impulses in lower cervical levels than in higher cervical levels for certain motion events. Interestingly, the data from this dynamic study showed that *both* the cranial (C2–C4) and caudal (C6–T1) CIVD levels exhibited greater and more comparable pressure values than those of the mid-spine disc level (C4–C6), and the pressure in upper/lower levels was ~four to six times higher than that of the

middle. We speculate that this phenomenon of higher CIVD pressure at both the upper and lower levels (as compared to that of the mid-spine) may be attributable to the "S" shape formed by the c-spine during the axial compression buckling motion. We speculate that during axial compression, the normal anatomical masses (i.e., the head and the torso) act on the c-spine "ends" act to increase the CIVD pressure in these levels, while the natural kyphotic to lordotic transition in cervical curvature paired with the transition of motion in the mid-spine during axial compression (i.e., point of reversal from extension in the upper to flexion in the lower c-spine) may act to dampen the CIVD response, thus accounting for the seemingly lower pressures in the mid-c-spine.

Results from this study (and our previous feasibility study [57]) align with this injury mechanism as well, in that the mid-cervical (C4–C6) CIVD levels exhibit the lowest pressure values, thus stressing the effect of transitional forces (i.e., shear) and moments at the mid-cervical region and lending credence to the hypothesized mechanism of injury. Despite these results, we recognize that changes in CIVD pressure alone are insufficient to infer injury risk, and that lower disc pressure is not necessarily indicative of lower injury risk in this region but does potentially reflect an important shift in injury mechanism. Further analysis of local kinematics (i.e., 3D motion tracking of individual cervical vertebrae), bending moments, and shear forces is planned to supplement the hypothesis that transitional curvature and shear-dominant loading is responsible for the experimental response. Unfortunately, the CIVD tissue response (i.e., changes in pressure) does not allow for shear analysis. As in previous studies, instrumentation for c-spine data capture is limited to force measurements captured at only the two farthest anatomical neck boundaries (i.e., load cells at the head and the torso/T1), thus making this analysis a persistent challenge. Thus, additional PMHS must be tested using this experimental technique in order to provide additional insight as to the cause of this occurrence.

Limitations were observed in this methodology pilot study. After reviewing the pilot experimentation data traces and comparing with previous studies [41], pressure sensor saturation issues were positively identified (i.e., experimental pressures greater than ~3450 kPa). These sensor saturations negatively affect peak pressure interpretation of the current pilot results in that peak pressure trends at the time of c-spine failure cannot be gleaned. Thus, saturated values were used primarily in a qualitative way to examine the pressure trends, and modifications (i.e., decreases) in drop height will be required in subsequent testing phases to maximize sensor capabilities. Additionally, the pressure sensors utilized in this testing are manually constructed, and variability in sensor response is a concern. It has come to light that slight differences in manufacturing may have resulted in slightly different dynamic ranges for each individual sensor (see Appendix D for individual pressure sensor calibration data). Prior to sensor use, a plausibility check was conducted to confirm pressure sensor calibration linearity; however, individual sensors were not cross validated against each other prior to implantation. Further sensor validation/testing utilizing a tensile machine and stepwise loading increases is planned to characterize the maximum ranges/capacities of each individual sensor. Results of validation testing will allow for strategic sensor selection and utilization to maximize data capture (e.g., sensors with the highest individual maximum capacities can be placed in the CIVD locations known to exhibit the higher trends in pressure during dynamic loading).

As in the preceding study, this methodology study's small sample size, paired with continued refinement of the experimental set-up, most likely affected the results. Basic interindividual/anatomical variability and/or subject-specific postural configurations (e.g., cervical sagittal balance) may also play a role in results [62]. Specimen quality and sensor grounding issues were identified during pilot testing and while successfully identified and mitigated, experimental pilot data from two of the four PMHS were not viable due to these

issues. Regarding specimen quality, as this was a pilot study with principally methodological intentions, we sought to maximize the anatomical gift of donation by utilizing PMHS that were available as a result of not being viable candidates for other testing. While two of the four subjects were deemed to have acceptable cervical vertebrae and IVDs with limited (age appropriate) degeneration, they still exhibited slightly suboptimal anatomical characteristics (e.g., normal postmortem changes, soft tissue desiccation, vertebral endplate changes, narrowing of the disc space/disc height) that most likely affected recorded CIVD pressures. Despite these limitations, our results suggest that obtaining CIVD pressure readings is possible, even in "imperfect" PMHS. Additional analysis of the 3D motion tracking data from this study is anticipated to provide supplementary information on subject-specific kinematics and pressure responses.

There have been questions related to the effect of pressure sensor location within the IVDs on sensor output [39,57]. Given the extremely small size of the cervical IVD (~15 mm diameter, ~5 mm anterior thickness [63]), perfect placement of the sensor in the center of the nucleus pulposus proves difficult. In a follow up to our previous work, the techniques for CIVD pressure sensor implantation were refined, and additional validation studies were conducted in order to better understand the behaviour of the pressure sensor data within the IVD tissue and in both quasistatic and dynamic environments (Appendix E). While proper sensor placement in the center of the IVD (i.e., inside the hydrostatic nucleus pulposus) is important for the trustworthiness of IVD pressure data, results of our validation study revealed that sensor output was not greatly affected by slight differences in sensor location within the center of the IVD. Because pressure is dependent on area and given the larger (i.e., lumbar spine) disc used in this validation study, slight variations in sensor positioning within the much smaller cervical discs may still affect the recorded pressures. This investigation is on-going.

As with any cadaveric-based study, the lack of active neck musculature in the PMHS may be viewed as a primary limitation. Musculature certainly contributes to both the stabilization of the neck and energy absorption during injurious insults to the c-spine. The effects of absent active musculature may be more pronounced in previous quasistatic experimentation [57]. However, this study included a dynamic test environment in which the PMHS c-spine was subjected to axial impact forces and concerns related to the lack of active musculature were mitigated by establishing a "neutral" plane and position in/to which the head/neck complex was allowed to drop. The rationale for limiting the tests to vertical impacts with the head/neck complex and torso all aligned in an anatomically neutral position was twofold; as highlighted in the Nightingale et al. studies: (1) the importance of active musculature is minimized during inverted/compressive loading, and (2) injuries sustained in this orientation/under these conditions occur two to three times more rapidly than the neck muscles can react and/or counteract the injurious forces to the c-spine [11]. Previous dynamic PMHS testing has shown that concerns related to the lack of active musculature are mitigated due to the timing of injury as it relates to muscle reflex timing—neck muscle reflex times (~50–65 ms for head loading [64]) exhibit a considerably longer duration than that required to produce c-spine injury in compressive head/neck impacts (5–18 ms) [11,12]. Thus, the effects of/lack of active musculature were mitigated in this test series by implementing the abovementioned rationale/experimental protocols as well as by removing limited soft tissue to maintain natural anatomical influence of surrounding structures (even if they are inactive). Tissue response conditions for current human surrogates for injury biomechanics testing (i.e., ATDs and HBMs) have been primarily defined from available (albeit limited) PMHS data; however, tissue response is dependent on test methodology resulting in highly variable results and leading to conflicting material properties and/or oversimplification of surrogate design. These limitations highlight the importance and

necessity of PMHS experimentation to better define the response of human tissues and to ultimately ensure that the surrogates are valid.

The "oversimplification" of a one-degree-of-freedom (i.e., vertical only) experimental protocol using isolated PMHS components (i.e., head and complete c-spine component PMHS versus whole body PMHS) is often considered a limitation [65,66]; however, we feel that this preliminary approach best correlates the results of previous work with the application of unique instrumentation, which is more aligned with current injury mitigation research and may better quantify the effects of forces on the human head/neck complex and the resultant injuries sustained in such dynamic environments. There exists promising translational relevance between potentially utilizing CIVD pressure as a biomechanical metric for assessing injurious axial loading and ATD/HBM development, as well as ongoing improvements in sports safety technology and injury prediction and prevention tools (e.g., sports helmet/padding designs, diving injury prevention, etc.). Future experimental directions include increasing specimen count for cervical level-specific injury tolerance development, incorporating multi-axis loading conditions (thus mimicking more of the "real world" environments in which humans are injured), and using CIVD pressure data to validate finite element HBMs.

5. Conclusions

This methodology study was an initial step in determining the potential applicability of CIVD pressures to assess the dynamic axial compression response of the human c-spine. This study establishes feasibility and assesses the promise of CIVD pressure as a biomechanical metric for assessing injurious axial loading and contributes a novel experimental framework for future injury tolerance research and model validation. Results confirm the feasibility of CIVD pressure response in investigating the transmission of load/forces along the entire c-spine (versus only at the anatomical limits), and the information provided has the potential for improving our understanding of c-spine loading. Limitations still exist in terms of exact values; however, the pressure responses recorded in this study provide valuable information for experimental parameters such as rates of CIVD pressure increase/decrease, peak pressures relative to specimen kinematics, and CIVD pressure/injury curve timing. Ongoing research into sports-related c-spine injuries resulting from dynamic axial (i.e., head-first) impacts contributes to the development of innovative safety technologies and injury prevention systems, injury countermeasures, and the design/improvement of proper human surrogates (i.e., ATDs/HMBs).

Author Contributions: Conceptualization, S.S., M.R.S. and F.J.L.-V.; methodology, S.S., M.R.S. and F.J.L.-V.; software, J.M.A.-G. and C.R.-M.G.; validation, S.S., M.R.S., J.M.A.-G. and C.R.-M.G.; formal analysis, S.S. and F.J.L.-V.; investigation, S.S., M.R.S., J.M.A.-G., C.R.-M.G. and F.J.L.-V.; resources, C.R.-M.G. and F.J.L.-V.; data curation, J.M.A.-G. and C.R.-M.G.; writing—original draft preparation, S.S.; writing—review and editing, S.S., J.M.A.-G., M.R.S. and F.J.L.-V.; visualization, S.S. and F.J.L.-V.; supervision, S.S., M.R.S. and F.J.L.-V.; project administration, S.S. and F.J.L.-V.; funding acquisition, F.J.L.-V. All authors have read and agreed to the published version of the manuscript.

Funding: This research was carried out with MOBIOS Lab, Institute for Research in Technology, Comillas Pontifical University resources. The work was supported by the call "Financiación Proyectos de Investigación Propios 2024" of the University, under the name "Assessment of Neck Loads in Head/Neck Motions within the Physiological Range". The views expressed here are solely those corresponding to the authors.

Institutional Review Board Statement: Not applicable.

Informed Consent Statement: Not applicable.

Data Availability Statement: The raw data supporting the conclusions of this article will be made available by the corresponding author upon request.

Acknowledgments: We would like to acknowledge all personnel at the MOBIOS Lab/Comillas Pontifical University who provided their assistance and expertise in the execution and analysis of these experiments, as well as the hospitality of R. Nightingale and J. Luck at Duke University (Durham, NC, USA). And lastly, for the altruistic gift of donor bodies, without which our research would not be possible.

Conflicts of Interest: The authors declare no conflicts of interest.

Abbreviations

The following abbreviations are used in this manuscript:

ATD	Anthropometric Test Device
CIVD	Cervical Intervertebral Disc
C-spine	Cervical spine
FSU	Functional Spinal Unit
HBM	Human Body Model
IVD	Intervertebral Disc
SCI	Spinal Cord Injury
PMHS	PostMortem Human Subject

Appendix A

Biomechanical studies establishing a relationship between CIVD tissue response (i.e., changes in pressure) and c-spine motion/loading.

Table A1. Comparison of primary biomechanical CIVD studies.

CIVD Study	Study Type		Subject Type		Instrumented CIVD Levels (n)	Experimental Conditions			Experimental Motions					
	In Vivo	In Vitro (PMHS)	Whole Body	Component		Quasistatic	Dynamic	Loading Mode	Flexion	Extension	Axial Rotation	Lateral Bending	Tension	Compression
Kambin et al. (1980) [43]	x		x [1]		*Exact levels undefined*	x		N/A *	N/A *	N/A *	N/A *	N/A *	N/A *	N/A *
Hattori et al. (1981) [42]	x		x [2]		C3C4 (4) C4C5 (18) C5C6 (36) C6C7 (22)	x		Manual (self/patient) manipulation ^	x	x	x	x	x	
Pospiech et al. (1999) [44]		x		x (c-spine) [3]	C3C4 (7) C5C6 (7)	x		Maximal moment ± 0.5 Nm, 10 N axial preload	x	x	x	x		
Cripton et al. (2001) [41]		x		x (FSU) [4]	C2C3 (2) C3C4 (1) C4C5 (1)	x		10 N/s under force control, up to 800 N						x
Sochor et al. (2025) [57]		x	x [5]		C3C4 (2) C5C6 (2) C7T1 (2)	x		Manual (physiotherapist) manipulation ^	x	x	x	x	x	x
Current Study		x		x (head/neck) [6]	Upper/C2C4 (2) Middle/C4C6 (2) Lower/C6T1 (2)		x	Inverted drop testing ~3.2 m/s						x

[1] (19) intraoperative patients undergoing cervical discectomies: (53) cervical discs. [2] (48) intraoperative patients undergoing cervical discectomies: (80) cervical discs. [3] (7) component PMHS c-spines (C2 through C7 only). [4] (4) PMHS cervical spine FSUs. [5] (2) whole body PMHS. [6] (2) component PMHS head/neck [cephalus with complete c-spine/through the fourth thoracic vertebrae (T4)]. * Not applicable, no loading/motion; predefined amounts of normal saline injected intradiscally to simulate CIVD pressure under muscle stress. ^ Neutral position (subject seated during testing).

Appendix B

Table A2. Results for c-spine testing show comparable data trends between MOBIOS experimentation and Nightingale et al. (1997) [11].

TEST *Rigid Surface*	Age, Sex	Velocity (m/s)	Angle (deg.)	Res. [a] Head Force (N)	Res. [a] Neck Force (N)	Axial [b] Neck Force (N)	Res. [c] Neck Force (N)	Time [d] (ms)	Injury Results
Nightingale et al. (1997) [11]									
N26-R+0	65, M	2.43	Vertex (0)	7638	4189	NI	NI	NI	• None
N24-R+0	62, M	3.20	Vertex (0)	8566	2643	1839	1973	2.2	• C1 two-part posterior arch fracture • C2 hangman's fracture (bilateral pars interarticularis fractures)
N22-R+0	71, M	3.26	Vertex (0)	8111	3010	1955	212	6.5	• C1 three-part comminuted fracture
Current Study									
PMHS 1 *	63, M	-	Vertex (0)	-	-	-	-	-	-
PMHS 2 **	63, M	-	Vertex (0)	-	-	-	-	-	-
PMHS 3	71, M	3.22	Vertex (0)	5704	1923	1751	1923	2.3	• C2 type II dens fracture • C2 left facet fracture (facet capsule intact)
PMHS 4	68, M	3.25	Vertex (0)	3845	1211	1145	1211	2.3	• C1 type III (Jefferson) fracture • C2 left transverse process fracture (through foramen) • C3 vertebral body and spinous process fracture(s)

NI, The specimen had No Injury. [a] Peak resultant force. [b] Magnitude of axial neck force at injury. [c] Magnitude of the resultant neck force at injury. [d] Elapsed time between impact and injury. * Specimen exhibited tissue degradation related to clinical treatment and thus acted as an experimental pilot only, drops × 2. ** Specimen demonstrated pre-existing injuries and thus acted as an experimental pilot only, drops × 2.

Appendix C

Appendix C.1. Individual Data Traces for PMHS 4 (0037M)

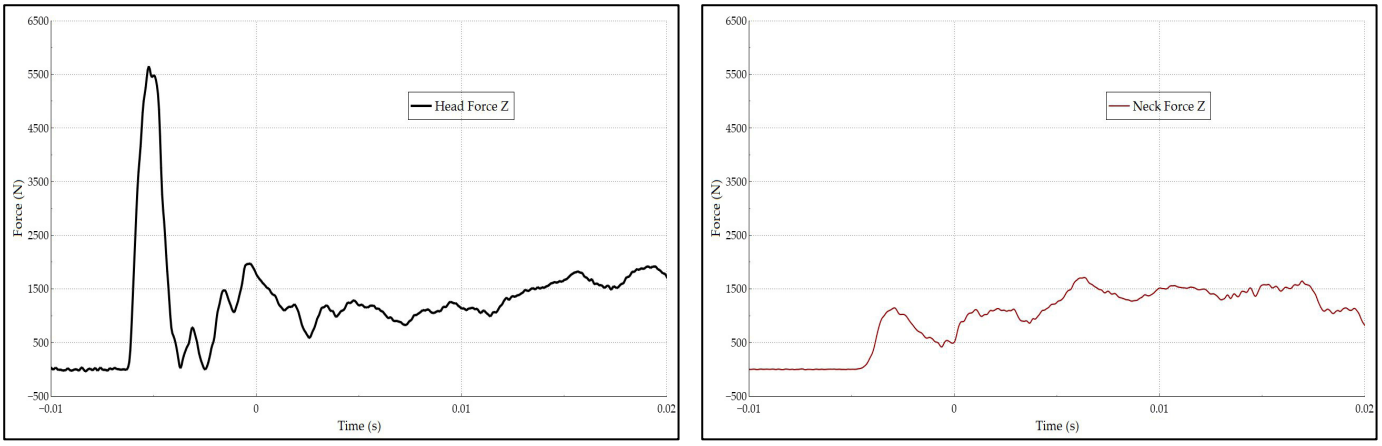

(**a**) (**b**)

Figure A1. *Cont.*

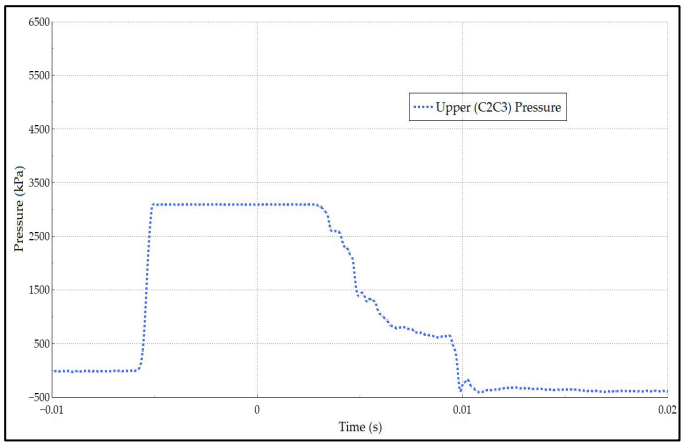

(**c**)

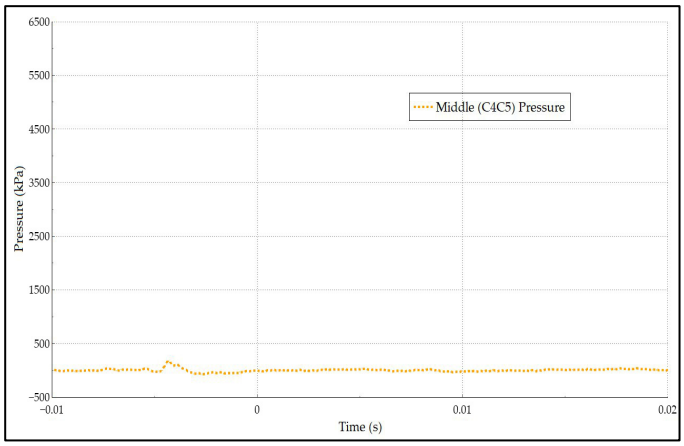

(**d**)

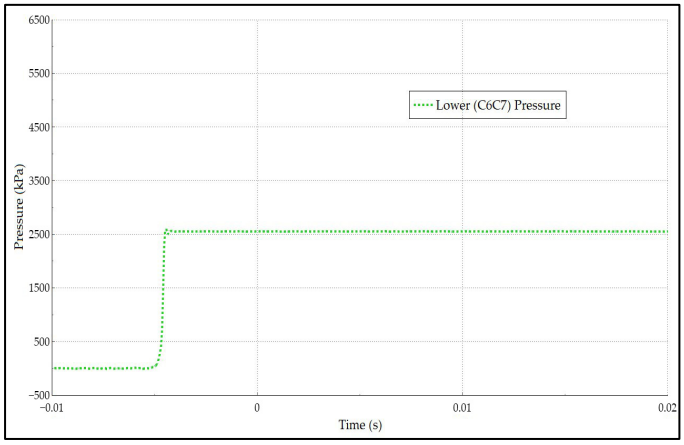

(**e**)

Figure A1. Individual data traces for PMHS 4 (0037M); head (**a**) and neck (**b**) force in Z, upper (**c**), middle (**d**), and lower (**e**) CIVD pressures.

Appendix C.2. Individual Data Traces for PMHS 3 (0038M)

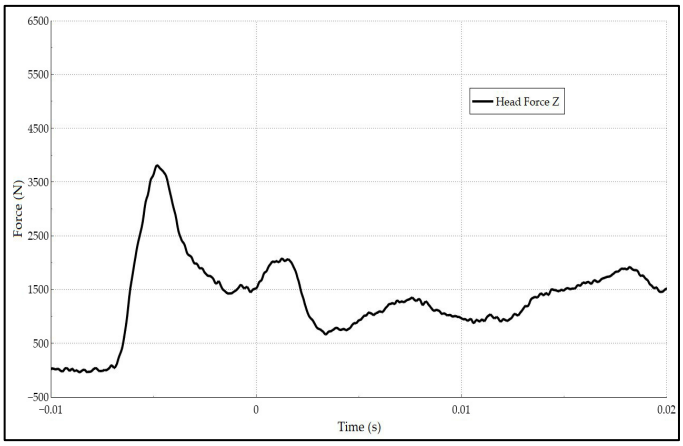

(**a**)

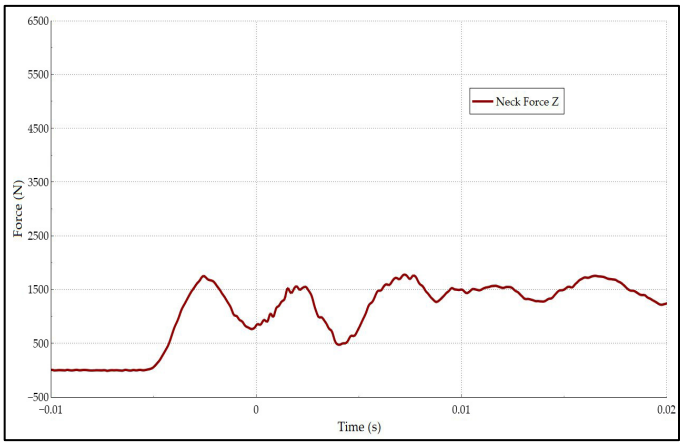

(**b**)

Figure A2. *Cont.*

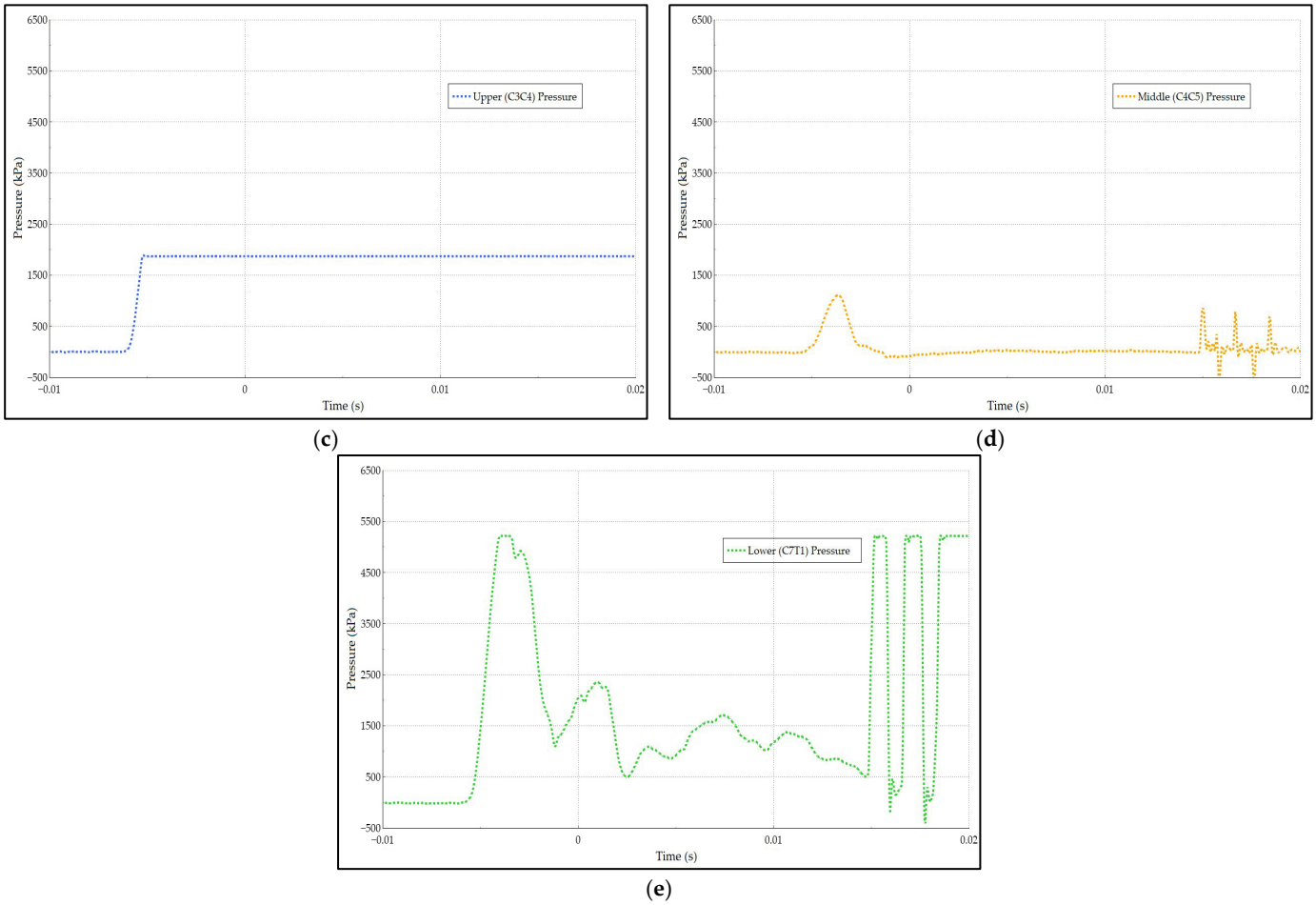

Figure A2. Individual data traces for PMHS 3 (0038M); head (**a**) and neck (**b**) force in Z, and upper (**c**), middle (**d**), and lower (**e**) CIVD pressures.

Appendix D

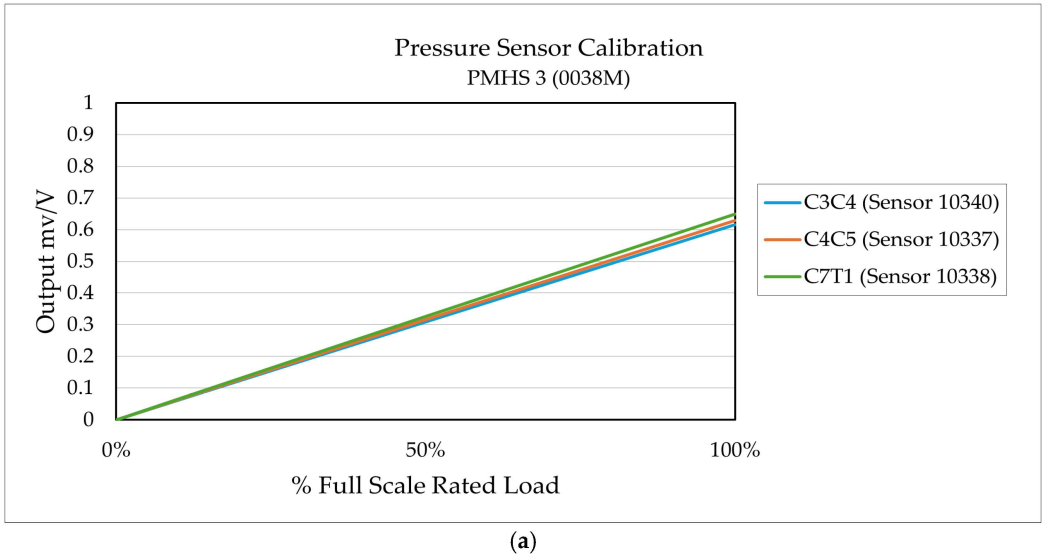

Figure A3. *Cont.*

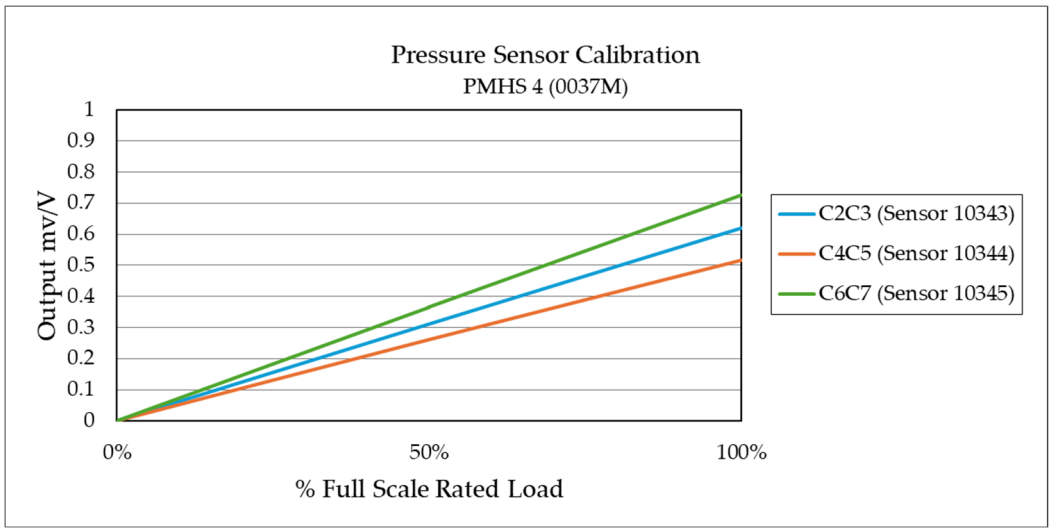

(**b**)

Figure A3. Sensor-specific calibration curves for PMHS 3 (0038M) (**a**) and PMHS 4 (0037M) (**b**). Each PMHS was instrumented with three miniature pressure sensors, with one sensor implanted at a location within each of three designated CIVD levels (i.e., upper/C2–C4 (blue), middle/C4–C6 (orange), and lower/C6–T1 (green)).

Appendix E

To investigate the effect of pressure sensor location on sensor output, a validation study was completed in which two pressure sensors were placed in two locations (anterior and posterior) within the nucleus pulposus of the *same* lumbar spine IVD (Figure A4).

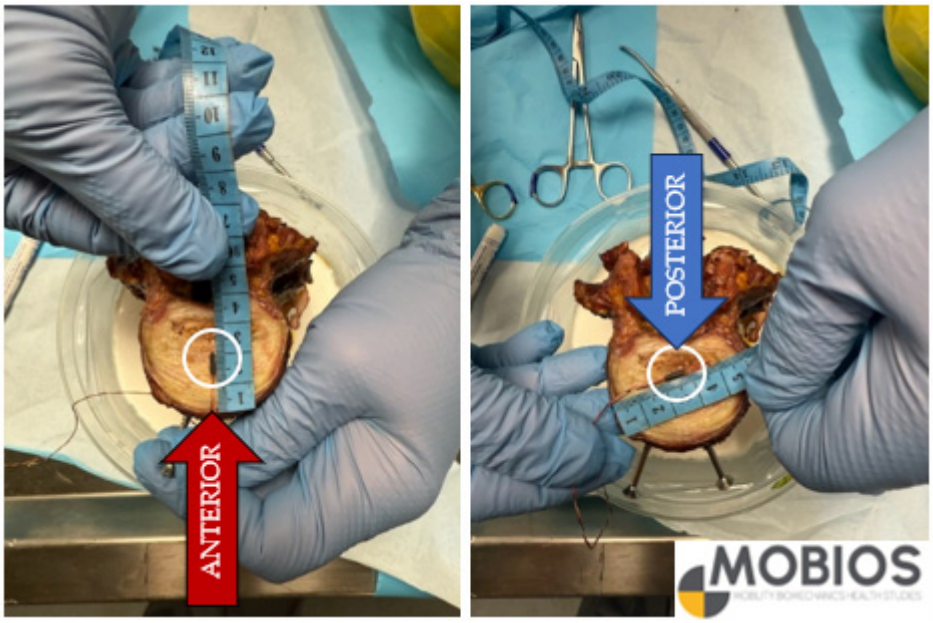

Figure A4. Validation study for IVD pressure sensor implantation/location; two pressure sensors (white circles) were placed in two locations (anterior and posterior) within a lumbar IVD to determine effect of location on pressure sensor output. Red = anterior sensor placement, blue = posterior sensor placement.

Results of validation study revealed that sensor output was not greatly affected by slight differences in sensor location within the IVD material in an IVD (Figure A5).

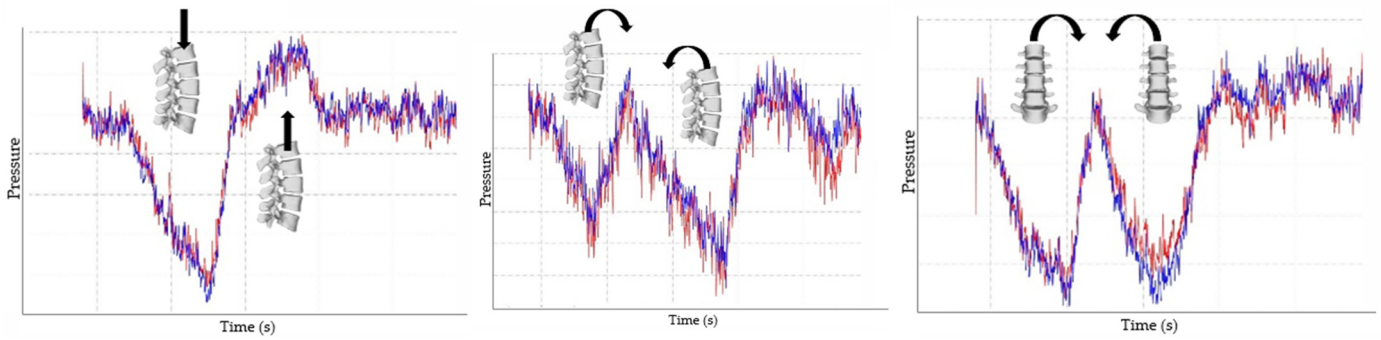

Figure A5. Experimental motions included lumbar spine (**a**) compression and tension, (**b**) flexion and extension, and (**c**) lateral flexion, left and right. Red = anterior sensor placement, blue = posterior sensor placement.

References

1. Myers, B.S.; Winkelstein, B.A. Epidemiology, Classification, Mechanism, and Tolerance of Human Cervical Spine Injuries. *Crit. Rev. Biomed. Eng.* **1995**, *23*, 307–409. [CrossRef]
2. Banerjee, R.; Palumbo, M.A.; Fadale, P.D. Catastrophic Cervical Spine Injuries in the Collision Sport Athlete, Part 1: Epidemiology, Functional Anatomy, and Diagnosis. *Am. J. Sports Med.* **2004**, *32*, 1077–1087. [CrossRef]
3. National Spinal Cord Injury Statistical Center. *The 2023 Annual Statistical Report (Complete Public Version) for the Spinal Cord Injury Model Systems*; National Spinal Cord Injury Statistical Center, University of Alabama at Birmingham: Birmingham, AL, USA, 2023.
4. Winkelstein, B.A.; Myers, B.S. The biomechanics of cervical spine injury and implications for injury prevention. *Med. Sci. Sports Exerc.* **1997**, *29*, 246.
5. Chan, C.W.; Eng, J.J.; Tator, C.H.; Krassioukov, A. Epidemiology of sport-related spinal cord injuries: A systematic review. *J. Spinal Cord Med.* **2016**, *39*, 255–264. [CrossRef]
6. McElhaney, J.; Snyder, R.G.; States, J.D.; Gabrielsen, M.A. Biomechanical Analysis of Swimming Pool Neck Injuries. *SAE Trans.* **1979**, *88*, 494–500.
7. Torg, J.S.; Vegso, J.J.; Sennett, B.; Das, M. The National Football Head and Neck Injury Registry: 14-Year Report on Cervical Quadriplegia, 1971 Through 1984. *JAMA* **1985**, *254*, 3439–3443. [CrossRef]
8. Hutton, M.J.; McGuire, R.A.; Dunn, R.; Williams, R.; Robertson, P.; Twaddle, B.; Kiely, P.; Clarke, A.; Mazda, K.; Davies, P.; et al. Catastrophic Cervical Spine Injuries in Contact Sports. *Glob. Spine J.* **2016**, *6*, 721–734. [CrossRef]
9. Burstein, A.H.; Otis, J.C.; Torg, J.S. Mechanisms and pathomechanics of athletic injuries to the cervical spine. *Athl. Inj. Head Neck Face* **1982**, *247*, 3266. [CrossRef]
10. Patel, S.A.; Vaccaro, A.R.; Rihn, J.A. Epidemiology of Spinal Injuries in Sports. *Oper. Tech. Sports Med.* **2013**, *21*, 146–151. [CrossRef]
11. Nightingale, R.W.; McElhaney, J.H.; Camacho, D.L.; Kleinberger, M.; Winkelstein, B.A.; Myers, B.S. The Dynamic Responses of the Cervical Spine: Buckling, End Conditions, and Tolerance in Compressive Impacts. *SAE Trans.* **1997**, *106*, 3968–3988.
12. Nightingale, R.W.; McElhaney, J.H.; Richardson, W.J.; Best, T.M.; Myers, B.S. Experimental Impact Injury to the Cervical Spine: Relating Motion of the Head and the Mechanism of Injury. *J. Bone Jt. Surg.* **1996**, *78*, 412–421. [CrossRef]
13. Association for the Advancement of Automotive Medicine. *The Abbreviated Injury Scale—2015 Revision*; AAAM: Des Plaines, IL, USA, 2016.
14. Kent, R.; Cormier, J.; McMurry, T.L.; Johan Ivarsson, B.; Funk, J.; Hartka, T.; Sochor, M. Spinal injury rates and specific causation in motor vehicle collisions. *Accid. Anal. Prev.* **2023**, *186*, 107047. [CrossRef]
15. Torg, J.S.; Guille, J.T.; Jaffe, S. Injuries to the Cervical Spine in American Football Players. *J. Bone Jt. Surg.* **2002**, *84*, 112. [CrossRef]
16. Torg, J.S.; Vegso, J.J.; O'Neill, M.J.; Sennett, B. The epidemiologic, pathologic, biomechanical, and cinematographic analysis of football-induced cervical spine trauma. *Am. J. Sports Med.* **1990**, *18*, 50–57. [CrossRef]
17. Bailes, J.E.; Petschauer, M.; Guskiewicz, K.M.; Marano, G. Management of Cervical Spine Injuries in Athletes. *J. Athl. Train.* **2007**, *42*, 126–134. [CrossRef]
18. Puvanesarajah, V.; Qureshi, R.; Cancienne, J.M.; Hassanzadeh, H. Traumatic Sports-Related Cervical Spine Injuries. *Clin. Spine Surg.* **2017**, *30*, 50. [CrossRef]
19. MacDonald, R.L.; Schwartz, M.L.; Mirich, D.; Sharkey, P.W.; Nelson, W.R. Diagnosis of Cervical Spine Injury in Motor Vehicle Crash Victims How Many X-rays Are Enough? *J. Trauma Inj. Infect. Crit. Care* **1990**, *30*, 392–397. [CrossRef]
20. Prasad, V.; Schwartz, A.; Bhutani, R.; Sharkey, P.; Schwartz, M. Characteristics of injuries to the cervical spine and spinal cord in polytrauma patient population: Experience from a regional trauma unit. *Spinal Cord* **1999**, *37*, 560–568. [CrossRef]

21. Hadley, M.N.; Sonntag, V.K.H.; Grahm, T.W.; Masferrer, R.; Browner, C. Axis Fractures Resulting from Motor Vehicle Accidents: The Need for Occupant Restraints. *Spine* **1986**, *11*, 861–864. [CrossRef]
22. Yoganandan, N.; Nahum, A.M.; Melvin, J.W.; The Medical College of Wisconsin Inc. on behalf of Narayan Yoganandan (Eds.) *Accidental Injury: Biomechanics and Prevention*; Springer: New York, NY, USA, 2015; ISBN 978-1-4939-1731-0.
23. Mertz, H.J.; Patrick, L.M. Strength and Response of the Human Neck. *SAE Trans.* **1971**, *80*, 2903–2928.
24. Huelke, D.F.; Mendelsohn, R.A.; States, J.D.; Melvin, J.W. Cervical Fractures and Fracture-dislocations Sustained without Head Impact. *J. Trauma Acute Care Surg.* **1978**, *18*, 533. [CrossRef] [PubMed]
25. Huelke, D.F.; Moffatt, E.A.; Mendelsohn, R.A.; Melvin, J.W. Cervical Fractures and Fracture Dislocations—An Overview. *SAE Trans.* **1979**, *88*, 462–468.
26. Nusholtz, G.S.; Huelke, D.E.; Lux, P.; Alem, N.M.; Montalvo, F. *Cervical Spine Injury Mechanisms*; SAE International: Warrendale, PA, USA, 1983.
27. Huelke, D.F.; Nusholtz, G.S. Cervical spine biomechanics: A review of the literature. *J. Orthop. Res.* **1986**, *4*, 232–245. [CrossRef] [PubMed]
28. Pintar, F.A.; Yoganandan, N.; Sances, A.; Reinartz, J.; Harris, G.; Larson, S.J. Kinematic and Anatomical Analysis of the Human Cervical Spinal Column Under Axial Loading. *SAE Trans.* **1989**, *98*, 1766–1789.
29. Nightingale, R.W. The Dynamics of Head and Cervical Spine Impact. Ph.D. Thesis, Duke University, Durham, NC, USA, 1993.
30. Myers, B.S.; Nightingale, R.W. Review: The Dynamics of Near Vertex Head Impact and its Role in Injury Prevention and the Complex Clinical Presentation of Basicranial and Cervical Spine Injury. *J. Crash Prev. Inj. Control* **1999**, *1*, 67–82. [CrossRef]
31. DeWit, J.A.; Cronin, D.S. Cervical spine segment finite element model for traumatic injury prediction. *J. Mech. Behav. Biomed. Mater.* **2012**, *10*, 138–150. [CrossRef]
32. Yoganandan, N.; Chirvi, S.; Pintar, F.A.; Banerjee, A.; Voo, L. *Injury Risk Curves for the Human Cervical Spine from Inferior-to-Superior Loading*; SAE International: Warrendale, PA, USA, 2018.
33. Lee, E.L.; Parent, D.; Craig, M.; McFadden, J.; Moorhouse, K. *Biomechanical Response Manual: THOR 5th Percentile Female NHTSA Advanced Frontal Dummy, Revision 2 (No. DOT HS 812 811)*; National Highway Traffic Safety Administration: Washington, DC, USA, 2020.
34. Parent, D.; Craig, M.; Moorhouse, K. *Biofidelity Evaluation of the THOR and Hybrid III 50th Percentile Male Frontal Impact Anthropomorphic Test Devices*; National Highway Traffic Safety Administration: Washington, DC, USA, 2017; p. 2017-22-0009.
35. Nachemson, A. Lumbar Intradiscal Pressure: Experimental Studies on Post-Mortem Material. *Acta Orthop. Scand.* **1960**, *31*, 1–104. [CrossRef]
36. Nachemson, A.; Morris, J.M. In Vivo Measurements of Intradiscal Pressure. Discometry, A Method For The Determination of Pressure In The Lower Lumbar Discs. *J. Bone Jt. Surg. Am.* **1964**, *46*, 1077–1092. [CrossRef]
37. Wilke, H.-J.; Neef, P.; Caimi, M.; Hoogland, T.; Claes, L. New In Vivo Measurements of Pressures in the Intervertebral Disc in Daily Life. Available online: https://oce.ovid.com/article/00007632-199904150-00005/HTML (accessed on 2 July 2024).
38. Richardson, R.; Donlon, J.; Chastain, K.; Shaw, G.; Forman, J.; Sochor, S.; Jayathirtha, M.; Kopp, K.; Overby, B.; Gepner, B.; et al. Test Methodology for Evaluating the Reclined Seating Environment with Human Surrogates. In Proceedings of the 26th International Technical Conference on the Enhanced Safety of Vehicles (ESV), Eindhoven, The Netherlands, 10–13 June 2019.
39. Burns, M.R.; Caldwell, A.J.; Shin, J.; Sochor, S.H.; Kopp, K.P.; Shaw, G.; Gepner, B.; Kerrigan, J.R. Assessing the Ability of Pressure Sensors Inserted into Intervertebral Discs to Detect Compression, Flexion, and Combined Flexion + Compression Loading. *SAE Int. J. Transp. Saf.* **2024**, *12*, 193–201. [CrossRef]
40. Nachemson, A.L. Disc Pressure Measurements. *Spine* **1981**, *6*, 93. [CrossRef]
41. Cripton, P.A.; Dumas, G.A.; Nolte, L.-P. A minimally disruptive technique for measuring intervertebral disc pressure in vitro: Application to the cervical spine. *J. Biomech.* **2001**, *34*, 545–549. [CrossRef]
42. Hattori, S.; Oda, H.; Kawaii, S. Cervical intradiscal pressure in movements and traction of the cervical spine. *Z. Orthop.* **1981**, *119*, 568–569.
43. Kambin, P.; Abda, S.; Kurpicki, F. Intradiskal Pressure and Volume Recording: Evaluation of Normal and Abnormal Cervical Disks. *Clin. Orthop. Relat. Res. 1976–2007* **1980**, *146*, 144. [CrossRef]
44. Pospiech, J.; Stolke, D.; Wilke, H.J.; Claes, L.E. Intradiscal pressure recordings in the cervical spine. *Neurosurgery* **1999**, *44*, 379–384; discussion 384–385. [CrossRef]
45. Gudavalli, M.R.; Potluri, T.; Carandang, G.; Havey, R.M.; Voronov, L.I.; Cox, J.M.; Rowell, R.M.; Kruse, R.A.; Joachim, G.C.; Patwardhan, A.G.; et al. Intradiscal Pressure Changes during Manual Cervical Distraction: A Cadaveric Study. *Evid. Based Complement. Altern. Med.* **2013**, *2013*, 954134. [CrossRef]
46. Dmitriev, A.E.; Cunningham, B.W.; Hu, N.; Sell, G.; Vigna, F.; McAfee, P.C. Adjacent level intradiscal pressure and segmental kinematics following a cervical total disc arthroplasty: An in vitro human cadaveric model. *Spine* **2005**, *30*, 1165–1172. [CrossRef]

47. Kretzer, R.M.; Hsu, W.; Hu, N.; Umekoji, H.; Jallo, G.I.; McAfee, P.C.; Tortolani, P.J.; Cunningham, B.W. Adjacent-level range of motion and intradiscal pressure after posterior cervical decompression and fixation: An in vitro human cadaveric model. *Spine* **2012**, *37*, E778–E785. [CrossRef]
48. Lou, J.; Li, Y.; Wang, B.; Meng, Y.; Gong, Q.; Liu, H. Biomechanical evaluation of cervical disc replacement with a novel prosthesis based on the physiological curvature of endplate. *J. Orthop. Surg.* **2018**, *13*, 41. [CrossRef]
49. Davies, M.A.; Bryant, S.C.; Larsen, S.P.; Murrey, D.B.; Nussman, D.S.; Laxer, E.B.; Darden, B.V. Comparison of cervical disk implants and cervical disk fusion treatments in human cadaveric models. *J. Biomech. Eng.* **2006**, *128*, 481–486. [CrossRef]
50. Lu, T.; Luo, C.; Ouyang, B.; Chen, Q.; Deng, Z. Effects of C5/C6 Intervertebral Space Distraction Height on Pressure on the Adjacent Intervertebral Disks and Articular Processes and Cervical Vertebrae Range of Motion. *Med. Sci. Monit. Int. Med. J. Exp. Clin. Res.* **2018**, *24*, 2533–2540. [CrossRef]
51. Lou, J.; Li, Y.; Wang, B.; Meng, Y.; Wu, T.; Liu, H. In vitro biomechanical comparison after fixed- and mobile-core artificial cervical disc replacement versus fusion. *Medicine* **2017**, *96*, e8291. [CrossRef] [PubMed]
52. Yan, Y.; Bell, K.M.; Hartman, R.A.; Hu, J.; Wang, W.; Kang, J.D.; Lee, J.Y. In vitro evaluation of translating and rotating plates using a robot testing system under follower load. *Eur. Spine J.* **2017**, *26*, 189–199. [CrossRef] [PubMed]
53. Bell, K.M.; Yan, Y.; Hartman, R.A.; Lee, J.Y. Influence of follower load application on moment-rotation parameters and intradiscal pressure in the cervical spine. *J. Biomech.* **2018**, *76*, 167–172. [CrossRef] [PubMed]
54. Whyte, T.; Barker, J.B.; Cronin, D.S.; Dumas, G.A.; Nolte, L.-P.; Cripton, P.A. Load-Sharing and Kinematics of the Human Cervical Spine Under Multi-Axial Transverse Shear Loading: Combined Experimental and Computational Investigation. *J. Biomech. Eng.* **2021**, *143*, 061013. [CrossRef]
55. Liu, Q.; Guo, Q.; Yang, J.; Zhang, P.; Xu, T.; Cheng, X.; Chen, J.; Guan, H.; Ni, B. Subaxial Cervical Intradiscal Pressure and Segmental Kinematics Following Atlantoaxial Fixation in Different Angles. *World Neurosurg.* **2016**, *87*, 521–528. [CrossRef]
56. Nightingale, R.W.; Myers, B.S.; Yoganandan, N. Neck Injury Biomechanics. In *Accidental Injury: Biomechanics and Prevention*; Yoganandan, N., Nahum, A.M., Melvin, J.W., Eds.; Springer: New York, NY, USA, 2015; pp. 259–308. ISBN 978-1-4939-1732-7.
57. Sochor, S.; Jiménez Octavio, J.R.; Carpintero Rubio, C.J.; Sochor, M.R.; Asensio-Gil, J.M.; Rodríguez-Morcillo García, C.; Lopez-Valdes, F.J. Human Cervical Intervertebral Disc Pressure Response During Non-Injurious Quasistatic Motion: A Feasibility Study. *Appl. Sci.* **2025**, *15*, 6167. [CrossRef]
58. Lopez-Valdes, F.J.; Mascareñas Brito, A.; Agnew, A.M.; Cripton, P.; Kerrigan, J.; Masouros, S.; Schmitt, K.-U.; Siegmund, G. The ethics, applications, and contributions of cadaver testing in injury prevention research. *Traffic Inj. Prev.* **2024**, *25*, 1115–1128. [CrossRef]
59. Matsushita, T.; Sato, T.B.; Hirabayashi, K.; Fujimura, S.; Asazuma, T.; Takatori, T. X-Ray Study of the Human Neck Motion Due to Head Inertia Loading. *SAE Trans.* **1994**, *103*, 1623–1632.
60. Nightingale, R.W.; Doherty, B.J.; Myers, B.S.; McElhaney, J.H.; Richardson, W.J. The Influence of End Condition on Human Cervical Spine Injury Mechanisms. *SAE Trans.* **1991**, *100*, 2040–2048.
61. Soltan, N.; Svensson, M.Y.; Jones, C.F.; Cripton, P.A.; Siegmund, G.P. In Vivo Pressure Responses of the Cervical Cerebrospinal Fluid in a Porcine Model of Extension and Flexion Whiplash Exposures. *Ann. Biomed. Eng.* **2025**, *53*, 1165–1179. [CrossRef]
62. Patwardhan, A.G.; Khayatzadeh, S.; Havey, R.M.; Voronov, L.I.; Smith, Z.A.; Kalmanson, O.; Ghanayem, A.J.; Sears, W. Cervical sagittal balance: A biomechanical perspective can help clinical practice. *Eur. Spine J.* **2018**, *27*, 25–38. [CrossRef]
63. Gilad, I.; Nissan, M. A Study of Vertebra and Disc Geometric Relations of the Human Cervical and Lumbar Spine. *Spine* **1986**, *11*, 154–157. [CrossRef]
64. Foust, D.R.; Chaffin, D.B.; Snyder, R.G.; Baum, J.K. Cervical Range of Motion and Dynamic Response and Strength of Cervical Muscles. *SAE Trans.* **1973**, *82*, 3222–3234.
65. Kerrigan, J.R.; Foster, J.B.; Sochor, M.; Forman, J.; Toczyski, J.; Roberts, C.W.; Crandall, J.R. Axial Compression Injury Tolerance of the Cervical Spine: Initial Results. *Traffic Inj. Prev.* **2014**, *15*, S238–S269.
66. Morgan, M.I.; Corrales, M.A.; Kaur, H.; Cripton, P.A.; Cronin, D.S. Importance of Neck Boundary Condition and Posture on Cervical Spine Response Assessed using a Detailed Finite Element Human Model in a Head-First Impact. *Ann. Biomed. Eng.* **2025**, *53*, 1931–1943. [CrossRef]